Original Article

High Performance Polymers

High Performance Polymers
1–10

DOI: 10.1177/0954008320945386
journals.sagepub.com/home/hip
SAGE

Ullmann coupling for low-cost synthesis of anthracene-based polyfluorenes: A photophysical approach

Deepika C Hasija[1], Vaijayanti D Ghase[1], Meenakshi M Rananaware[1,2] and Vishwanath R Patil[1]

Abstract

A set of anthracene containing polyfluorenes (PFs) having 9,10-diphenylanthracene with alkyl substituents and aniline containing fluorenes were prepared. Commonly, light-emitting polymers were synthesized using expensive palladium-like catalysts. In the present work, palladium was replaced by copper as a cost-effective PF synthesis catalyst, which is also suitable for large-scale polymer synthesis. Synthesized PFs emit light in the blue region with a bandgap of 2.87–2.90 eV. Thermally stable PFs had a decomposition temperature of more than 305°C and a glass transition temperature of 125–138°C. PFs were soluble in organic solvents and had a molecular weight of around 21,700–25,500. The electrochemical study of these PFs showed low level of highest occupied molecular orbital (HOMO) energy of −5.16 to −5.26 eV, which was significantly higher than that of PF (5.7 eV). These findings suggested that the resulting PFs could be used as a component of the light-emitting diode.

Keywords

Polyfluorenes, Ullmann coupling, 9, 10-diphenylanthracene, light-emitting polymers, cyclic voltammetry

Introduction

After the first discovery of luminescence in poly (para-phenylenevinylene),[1] significant research has been done on the development of conjugate materials for display applications. Conjugated polymers have found wide-ranging applications because of their advantages, such as large-scale electronic devices, low cost and lightweight.[2–7] In the past few years, the exponential growth of luminescent polymers has opened new doors for conjugated polymer synthesis. Owing to the increased use of transition-metal catalysis, the polymer systems, which were difficult to synthesize, are now possible in recent years. Palladium[8–16] is the commonly used metallic catalyst for the synthesis of conjugated polymers. Nickel[17–19] and rhodium[20–22] are a few other examples of the transition metals used for the synthesis of conjugated polymer. The use of copper for polymerization was not explored although it was the oldest transition metal that was used as the catalyst. Copper-catalyzed polymerization is a good method, as this does not involve organometallic monomers otherwise needed for conventional palladium-involved cross-coupling reactions. This not only reduces the number of steps involved but also reduces the unwanted metal waste generated after synthesis of polymers. Reducing the number of steps makes this method more economical and eco-friendly.[23,24] Hence, in this work, we explored low-cost synthesis of conjugated polyfluorenes (PFs) using Ullmann coupling catalyzed by copper.

The reason for selecting PFs was that over the past few years, PFs have proven promising for their use as blue light-emitting diodes (LEDs). Due to its strong photoluminescence (PL) quantum yields, and large bandgaps, PFs as emitters are of particular importance.[25–27] Nevertheless, their key concern is the low-wavelength emission obtained due to their propensity to decompose structurally over time at higher temperature in solid state, which induces color instability when integrated into the LEDs.[28,29] Interestingly, substituting aryl groups at fluorene's C-9 position not only

[1] Department of Chemistry, University of Mumbai, Santacruz (E), Mumbai, Maharashtra, India
[2] Dwarkadas Jivanlal Sanghvi College of Engineering, Vile Parle (W), Mumbai, Maharashtra, India

Corresponding author:
Vishwanath R Patil, Department of Chemistry, University of Mumbai, Santacruz (E), Mumbai 400 098, Maharashtra, India.
Email: vishwanathrpatil03@gmail.com

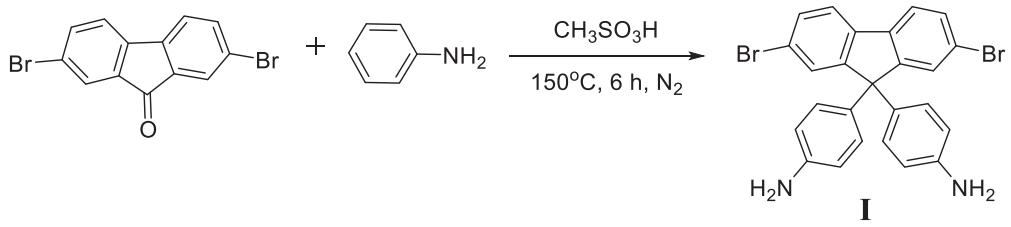

Figure 1. Synthesis of FDA. FDA: 4,4′-(2,7-dibromo-9H-fluorene-9,9-diyl) dianiline.

improves solubility but also enables the challenge of stability to be solved and decreases interchain interactions, which improves both the optical and electronic properties of polymers.[30] Arylamines are commonly used as a hole-transporting material in LEDs.[31–35] Previous reports show that substituting triarylamine moieties at the 9-position of fluorene-based polymers results in good quantum efficiency and low ionization potential.[36,37]

Furthermore, anthracene derivatives have also found a wide variety of uses in chemical, photographic, and medical applications.[38–41] Provided their excellent stability and fluorescence, anthracene-based compounds are commonly used in organic light-emitting diode (OLED) applications.[42] Recently, thermally activated delayed fluorescence and OLED efficiency enhancement experiments via triplet fusion have generated even more interest in anthracenes.[43–45] Although the use of triphenylamine as blue-emitting materials has been documented, the use of phenylamine substituted fluorene moiety and 9,10-diphenylanthracene (DPA) as copolymers emitting in the blue region is not known to our knowledge. Therefore, our aim was to use Ullmann coupling to synthesize copolymers emitted in the deep blue region.[23,24] We also emphasize the low-cost copper-catalyzed synthesis of polymers with relatively high molecular weight and strong thermal and optical properties.[46–48]

Experimental procedure

Materials

Chemicals were obtained from SD Fine Chemicals Limited (Mumbai, Maharashtra, India) and Sigma Aldrich (Mumbai, Maharashtra, India). 2,7-Dibromo-9H-fluorene, aniline, magnesium, *p*-bromo anisole, 2-methyl anthraquinone, 2-ethyl anthraquinone, 2-*tert* butyl anthraquinone, boron tribromide, copper iodide, picolinic acid, and ferrocene were obtained from Sigma Aldrich. Methanesulfonic acid, stannous chloride, sodium sulfate, tetrahydrofuran, silica gel, and bromobenzene were obtained from SD Fine Chemicals Limited. All reactions were performed in dry conditions in the presence of nitrogen for moisture-sensitive compounds. Solvents have been purified by the methods reported. Spectroscopic-grade tetrahydrofuran (THF) was used in absorption and emission studies. 2, 7-Dibromofluorenone was synthesized using the reported method.[49]

Characterization

A Bruker (Switzerland) nuclear magnetic resonance (NMR) spectrometer (AMX-300) was used to record NMR spectra with tetramethylsilane as the internal standard. Spectrophotometer of the Perkin-Elmer (USA) 1600 series was used to record Fourier transform infrared (FTIR) spectra. LS55 luminescence spectrometer was used to record PL spectra. Thermogravimetric experiments were conducted on the Perkin-Elmer thermal analyzer under the nitrogen atmosphere. X-ray diffractogram was obtained using the Shimadzu XRD-7000 X-ray diffractometer with Cu (K_α) ($\lambda = 1.542$ Å). Polymer molecular weight was determined using a Perkin Elmer 200 GPC series. THF was used as a solvent and polystyrene were utilized as the standard for calibration. Cyclic voltammetry (CV) was recorded on an ADC 164Autolab, and 0.1 M tetrabutylammonium hexafluorophosphate was used as the supporting electrolyte dissolved in CH_2Cl_2. Glassy carbon was used as the working electrode. Along with internal standard Ferrocene/ferrocenium (Fc/Fc+), Pt and Ag/AgCl electrodes were also used as counter and reference electrodes, respectively.

Monomer and polymer synthesis

*Synthesis of 4,4′-(2,7-Dibromo-9H-fluorene-9,9-diyl) dianiline) (**I**).* 4,4′-(2,7-Dibromo-9H-fluorene-9,9-diyl) dianiline) (**I**) (FDA) was synthesized using a procedure reported.[46–48,50] The general reaction scheme is shown in Figure 1.

Proton nuclear magnetic resonance (^{1}H NMR) (300 MHz, $CDCl_3$): $\delta = 7.53$ (d, 2 H), 7.43 (m, 4 H), 6.92 (d, 4 H), 6.56 (d, 4 H), 3.63 (s, 4 H). Carbon-13 nuclear magnetic resonance (^{13}C NMR) (75 MHz, $CDCl_3$): $\delta = 64.26$, 115.01, 120.41, 121.69, 128.95, 129.27, 130.52, 134.4, 137.83, 145.32, 145.66, 154.15. IR (cm^{-1}): 3452–3338 (N–H, stretching), 3032 (C–H, stretching), 1618 (N–C, bending), and 1051 (C–Br stretching). MS m/z calculated for $C_{25}H_{18}Br_2N_2$ 506.2; found 507. Analysis calculated for

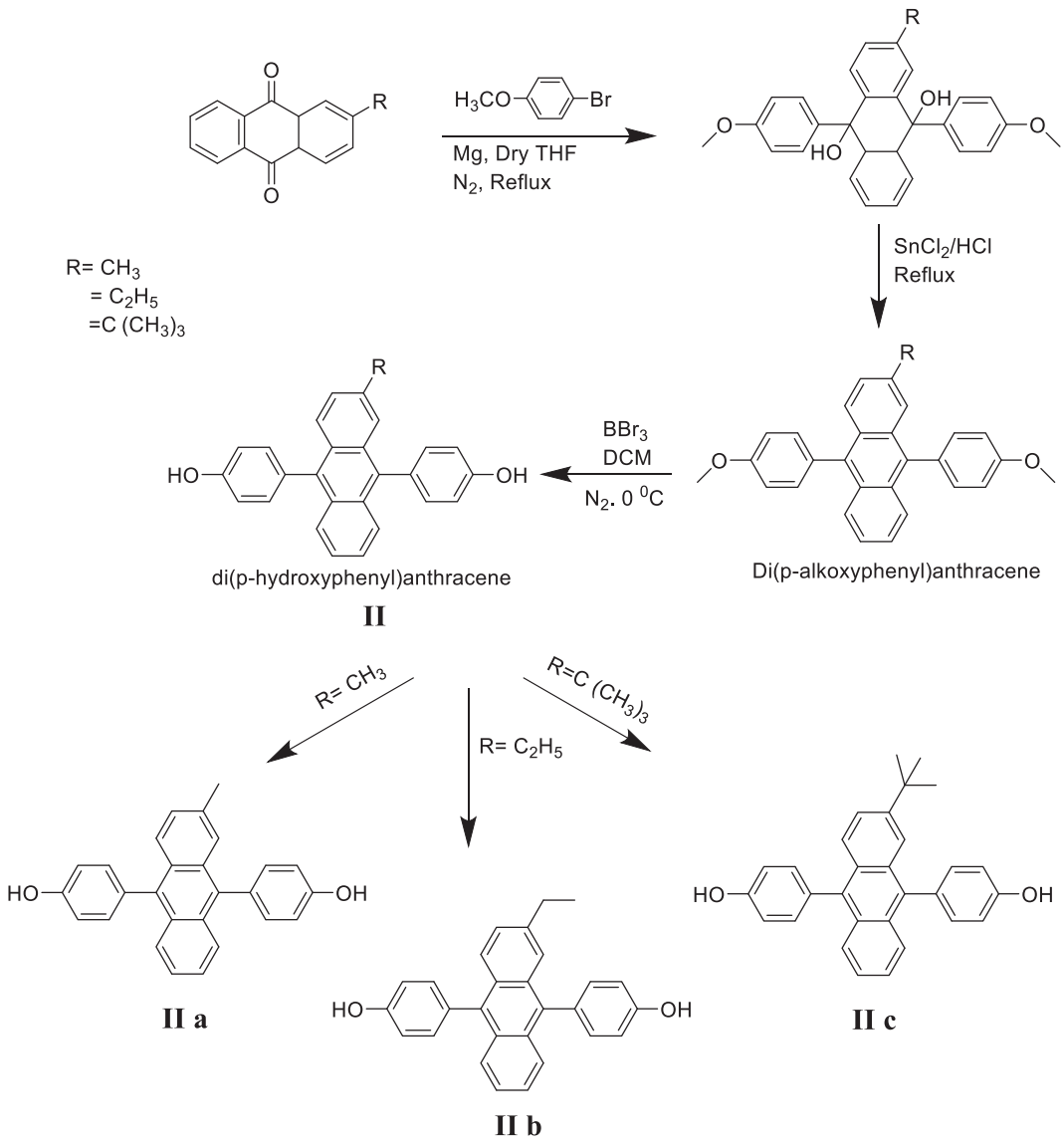

Figure 2. Synthesis of 2-alkyl-9,10-di(*p*-hydroxyphenyl) anthracene.

$C_{25}H_{18}Br_2N_2$: C, 59.29; H, 3.61; N, 5.55. Found: C, 59.32; H, 3.53; N, 5.52%.

*Acene containing monomer (**II**).* The alkyl-substituted 9,10 DPA **(II)** has been synthesized according to the literature reports.[51–55] Figure 2 and Figure S1 show the reaction scheme and the experimental procedure for the synthesis of the acene monomers **(II)**.[46–48]

Polymerization. The copolymerization of monomer **I** with monomer **II** was performed to obtain the desired PFs using copper iodide as a catalyst.[56] Figure 3 shows the polymerization reaction. For polymer synthesis, in dry flask picolinic acid (55 mg, 0.40 mmol), CuI (15 mg, 0.20 mmol), FDA (I) (2.0 mmol), II (2.0 mmol), and potassium phosphate (0.544 g, 4.0 mmol) were mixed in dimethyl sulfoxide (4.0 mL). The reaction mixture was strongly stirred in the oil bath, held at 85°C for 24 h. End capping of the –OH groups using bromobenzene was achieved. After cooling, this reaction mass was then poured to a mixture of water (4 mL) and ethyl acetate (40 mL). After the removal of the organic layer, the aqueous part was separated by ethyl acetate (40 mL). After being dried with sodium sulfate, the organic layer was passed through silica gel. The organic layer was dissolved in methanol and precipitated to get the desired polymer. The yield of the resulting brown colored polymer was around 65–70%.[46–48] Using a similar scheme, series of the FDA-diphenylacene polymers P1, P2, and P3 were synthesized.

Poly (FDA-MDPA) (**P1**): IR (KBr): 3358 (N–H, stretch), 2950 (C–H, aromatic), 1660 (N–H bend), 1510 (C=C aromatic), 1246 (C–O–C linkage), 1240 (C–N stretch) cm^{-1}; ^1H NMR (300 MHz, $CDCl_3$, δ ppm): 1.28 (s, 3 H, $–CH_3$), 3.69 (s, 4 H, $–NH_2$) 6.54–7.48 (m, Ar–H); ^{13}C NMR (75

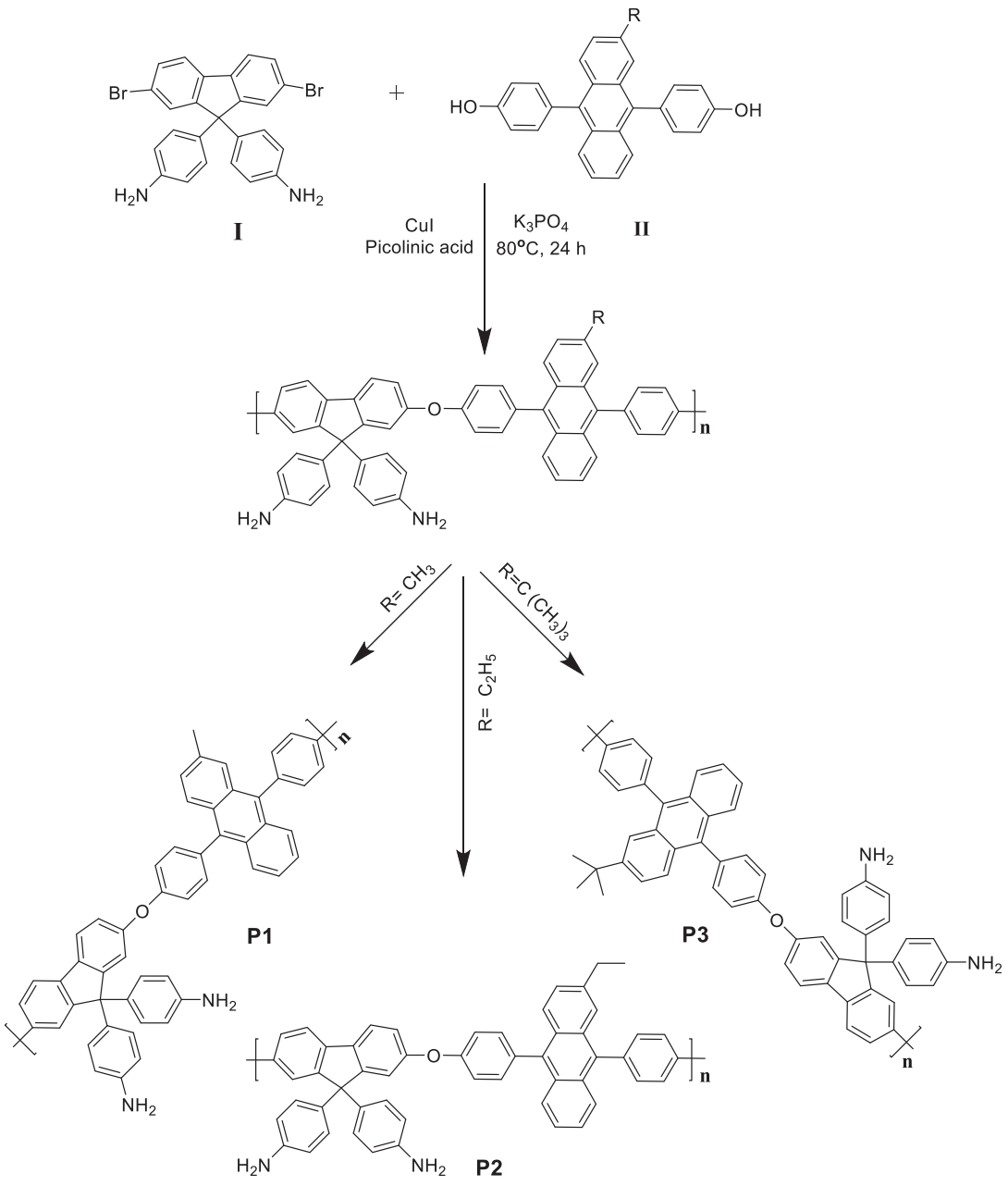

Figure 3. Synthesis of polymers.

MHz, $CDCl_3$, δ ppm): 31.56 ($-CH_3$), 64.24 (aliphatic carbon), 113.33–142.14 (aromatic carbon).

Poly (FDA-EDPA) (**P2**): IR (KBr): 3347 (N–H, stretch), 2956 (C–H, aromatic), 1654 (N–H bend), 1506 (C=C aromatic), 1248 (C–O–C linkage), 1228 (C–N stretch) cm^{-1}; ^1H NMR (300 MHz, $CDCl_3$, δ ppm): 1.12 (t, 3 H, $-CH_3$), 2.68 (q, 2 H, $-CH_2$), 3.69 (s, 4 H, $-NH_2$), 7.16–8.32 (m, 74 H, Ar–H), 2.38 (s, 12 H, $-CH_3$); ^{13}C NMR (75 MHz, $CDCl_3$, δ ppm): 15.31 ($-CH_3$), 29.15 ($-CH_2$), 64.29 (aliphatic carbon), and 115.08–163 (aromatic carbon).

Poly (FDA-TDPA) (**P3**): IR (KBr): 3347 (N–H, stretch), 2956 (C–H, aromatic), 1660 (N–H bend), 1510 (C=C aromatic), 1248 (C–O–C linkage), 1234 (C–N stretch) cm^{-1}; ^1H NMR (300 MHz, $CDCl_3$, δ ppm):1.26 (s, 9 H, $-CH_3$), 3.69 (s, 4 H, $-NH_2$), 6.54–7.49 (m, Ar–H); ^{13}C NMR: (75 MHz, $CDCl_3$, δ ppm): 30.61 ($-CH_3$), 34.91 (*tert* carbon), 56.49 (carbon of $-OCH_3$), 64.33 (aliphatic carbon), and 113.31–142.14 (aromatic carbon).

Result and discussion

Structural characterization

The synthesis of polymer was confirmed by ^1H NMR, ^{13}C NMR, and FTIR spectroscopy. The spectra of conjugated

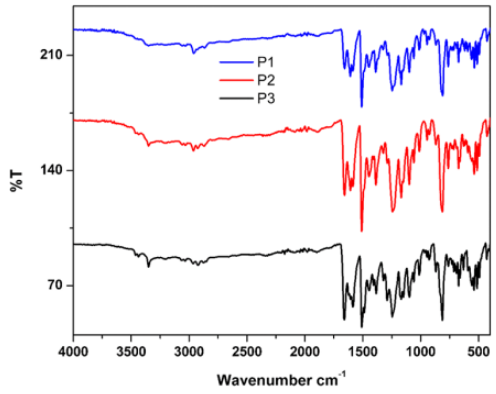

Figure 4. FTIR spectra of polymers. FTIR: Fourier transform infrared.

polymers were very complicated due to the existence of various bands of different intensities. The most important characteristic of the FTIR spectra of polymers (Figure 4) was the absence of the broad absorption peaks at around 3300 cm^{-1}, suggesting the termination of the hydroxyl end group of alkyl-substituted DPA monomers and completion of the polymerization.

The NMR spectra of polymers consisted of overlapping signals. The ^{1}H NMR spectrum of polymers showed signals in both aliphatic and aromatic region. The signal for aliphatic protons was observed between 0 and 3.6 δ ppm, while aromatic protons showed signals from 6.5 to 7.5 δ ppm. The signal due to –OH group of anthracene monomer was not present in the spectrum, suggesting that the

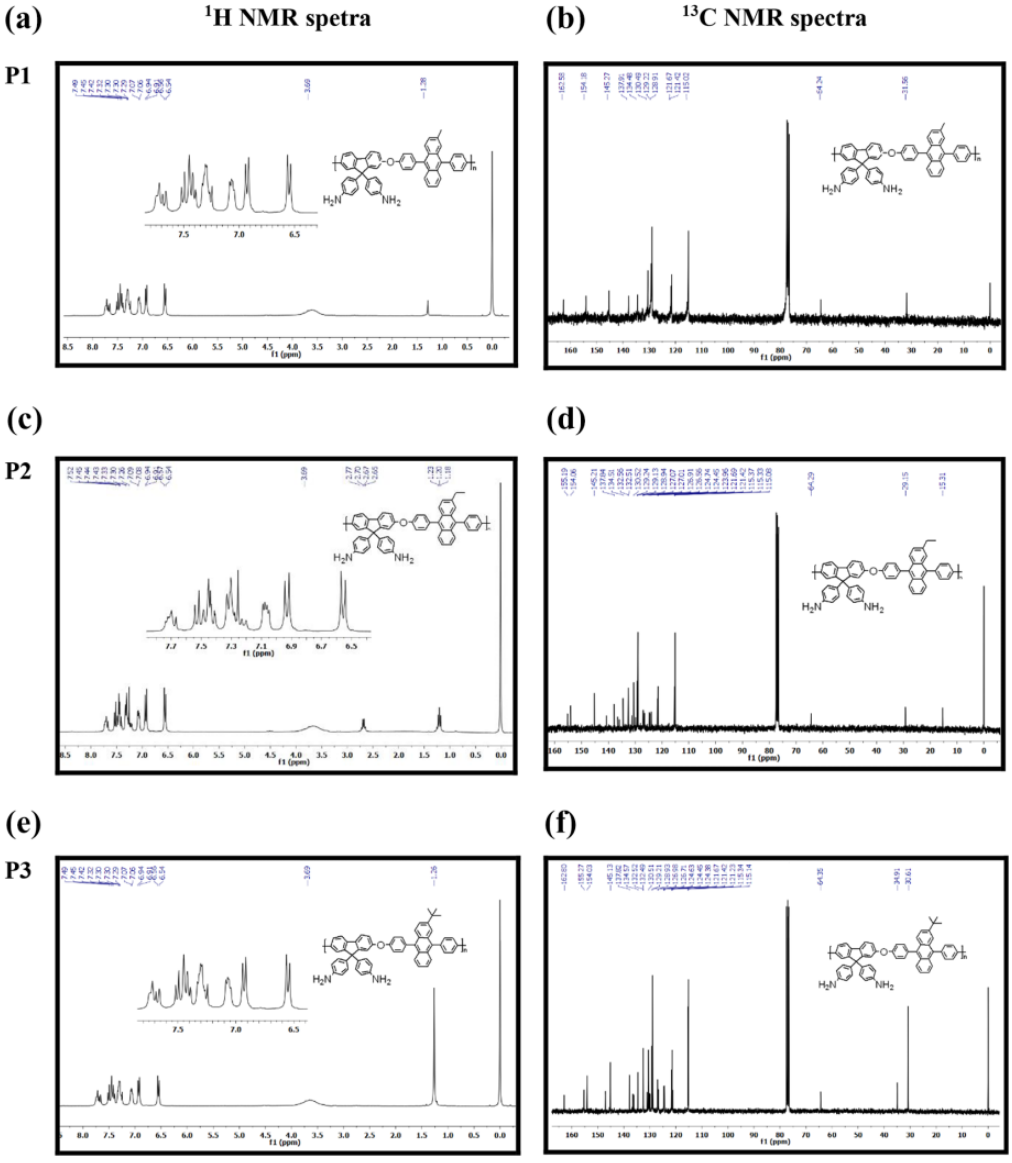

Figure 5. (a) ^{1}H NMR and (b) ^{13}C NMR spectra of polymers. ^{1}H NMR: proton nuclear magnetic resonance; ^{13}C NMR: carbon-13 nuclear magnetic resonance.

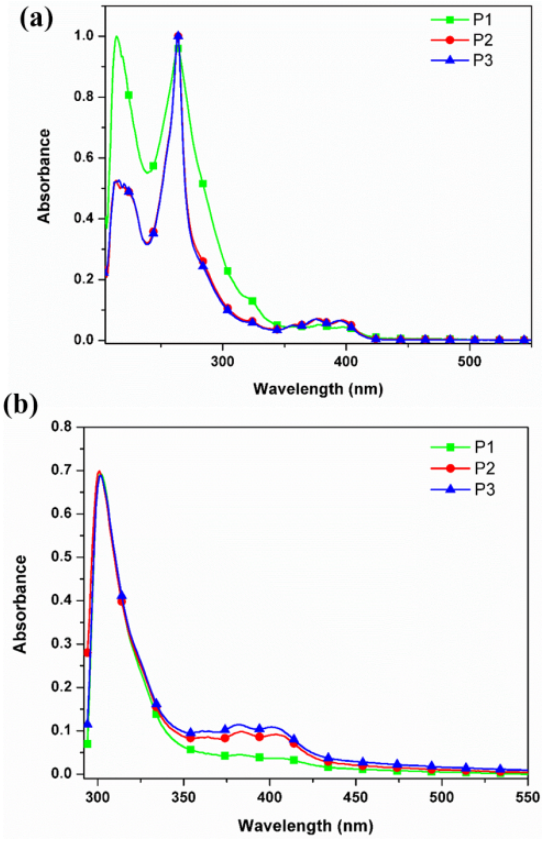

Figure 6. UV-visible absorption spectra of polymers in (a) solution and (b) solid film. UV: ultraviolet.

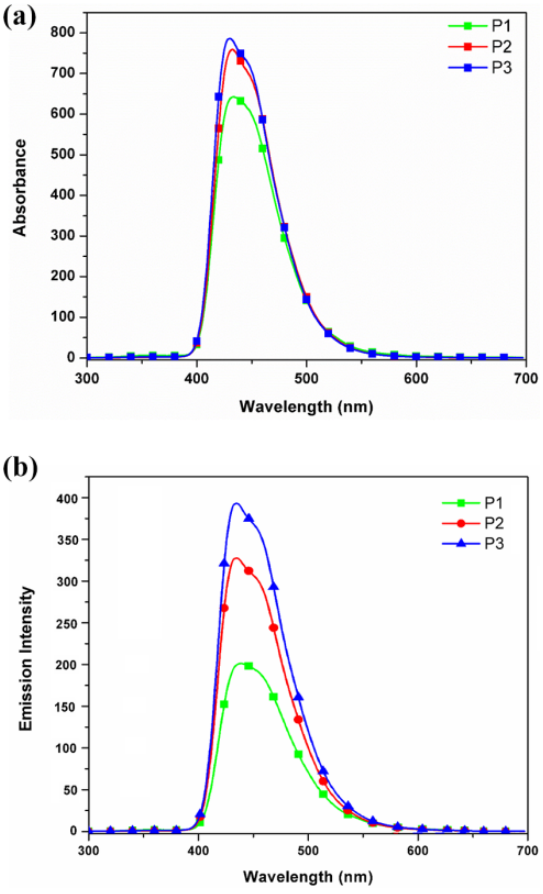

Figure 7. Photoluminescence spectra of polymers in (a) solution and (b) solid film.

polymerization was completed via removal of HBr molecule. The ^{1}H and ^{13}C NMR spectra are shown in Figure 5.

Optical studies

Figures 6 and 7 show ultraviolet (UV)-visible and PL spectra of polymer in the solvent and film, respectively. THF was used to record both absorption and emission spectra of the polymers. To obtain a homogeneous film, a thin layer was spin-coated from $CHCl_3$ solution for the absorption and emission spectra of the solid film. The spectroscopic data for solid film and solution are listed in Table 1.

The solution's absorption spectra showed two large bands in the region of 200–270 nm due to π–π* transition. The nature of absorption of spectra for solid films and solutions was very close. According to the literature, the 9,9 dialkyl fluorene exhibits absorption at 390 nm, and anthracene displays three absorption peaks at 359, 377, and 396 nm.[57] The shoulder that was observed at around 400 nm was due to anthracene group absorption and was separated from the substituents. A redshift was observed for the polymer thin film as opposed to the solution due to some aggregation in the solid film. The optically measured bandgap was 2.87–2.90 eV, which was similar to the optical bandgap of the blue-emitting materials. A wide bandgap is required for a material to be used as a blue-light emitter. The results showed that PFs with alkyl side groups have no effect on its polymer E_g. The polymers showed substantial PL in both the solid and solution resulting in pure blue emissions with a wavelength of around 430 nm on UV excitation. There was practically no blue PF emission normally observed at around 420 nm. Therefore, emission obtained was only due to the acene units in the main PF chain. The generated excitons were transferred entirely from the fluorene chain to the acene moieties. The excimer emission has also not been observed in the films.[58] The

Table 1. Optical properties of polymers.

	UV absorption (λ_{max} (nm))		PL (λ_{max} (nm))		ϕ (%)[a]	
Polymer	THF	Film	THF	Film	THF	Film
P1	263, 378, 399	300, 383, 408	442	449	56	11
P2	263, 376, 397	300, 383, 404	434	441	72	18
P3	264, 375, 401	300, 383, 402	427	435	80	23

UV: ultraviolet; PL: photoluminescence.
[a]Measured using 9,10-DPA as standard.

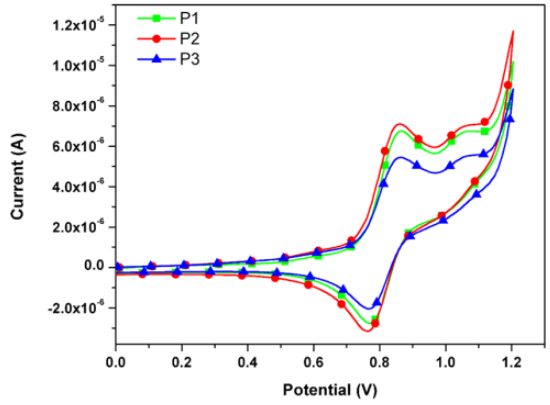

Figure 8. Cyclic voltammograms o f polymers.

emission spectrum of the solids and the solution was almost identical. This may be attributed to the obstructed intermolecular interaction due to the distorted anthracene and fluorene-substituted framework. Due to aggregation of the polymer in solid film, redshifts (7–8 nm) were observed in the emission spectra of solid films. The data for thin films suggested a low aggregation. The aryl chains on the fluorene units probably prevent the molecules from stacking and thus led to low aggregation.[59] The band for absorption was wider than the band for emissions. Using DPA as standard, the fluorescence quantum yield obtained was 56–80% in solution and 11–23% in solid films. Aggregation in the solid films and quenching allow the solid layer to decrease the quantum yields. Though the PL spectra of the polymer were red-shifted in thin film, they remained blue emitters in the solid state. Therefore, due to their high E_g and blue PL emissions, the thin film of polymers can be promising for its use as a host in polymer Light-emitting diode (PLEDs).

Electrochemical studies

CV was carried out to study the electrochemical properties of the polymers, as shown in Figure 8. The electrolyte *n*-Bu_4NBF_4 (0.1 M) was dissolved in CH_2Cl_2 and the scanning rate maintained was of 100 mV/s. The redox couple ferrocene–ferrocenium calibration was done having an energy level below the 4.8 eV vacuum levels. The voltammograms of the polymers exhibited a quasi-reversible curve, which was relatively long. The findings suggested that the highest occupied molecular orbital (HOMO) and LUMO energy levels had substantially evolved on the introduction of anthracene unit in the main polymer backbone. The peak potentials of oxidation (E_{ox}) for the polymers were 0.74, 0.74, and 0.75 eV, respectively. The energy levels of HOMO and LUMO were measured and estimated at −5.14, −5.14, and −5.15 eV for HOMO, and −2.27, −2.27, and −2.25 eV for LUMO levels, respectively. The values were quite similar to *N*, *N*′-(3-methyl phenyl)-1,1′-biphenyl-4,4′-diamine and *N*, *N*′-di(1-naphthyl)-*N*, *N*′-diphenyl(1,1′-biphenyl)-4,4′-diamine, which are widely used materials. In Table 2, we summarize the electrochemical properties of all polymers.

Table 2. Electrochemical properties of polymers.

Polymer	E_g (eV)[a]	E_{ox} (eV)[b]	E_{HOMO} (eV)[c]	E_{LUMO} (eV)[d]
P1	2.87	0.74	−5.14	−2.27
P2	2.89	0.74	−5.14	−2.25
P3	2.90	0.75	−5.15	−2.25

[a]The edge of UV spectrum in thin-film state.
[b]Onset oxidation potential.
[c]The equation $E_{HOMO} = -(E_{ox} + 4.4)$.
[d]The equation $E_{LUMO} = E_{HOMO} - E_g^{opt}$.

Table 3. Molecular weights and thermal analysis data of polymers.

Polymer	M_n[a]	M_w[a]	PDI (M_w/M_n)	T_d (°C)[b]	T_g (°C)
P1	12670	24,200	1.91	283	125
P2	11,900	21,700	1.82	270	127
P3	11,600	25,500	2.2	305	138

TGA: thermogravimetric analysis.
[a]Determined by gel permeation chromatography (GPC) in THF using polystyrene standards.
[b]10% weight loss temperature by TGA under N_2.

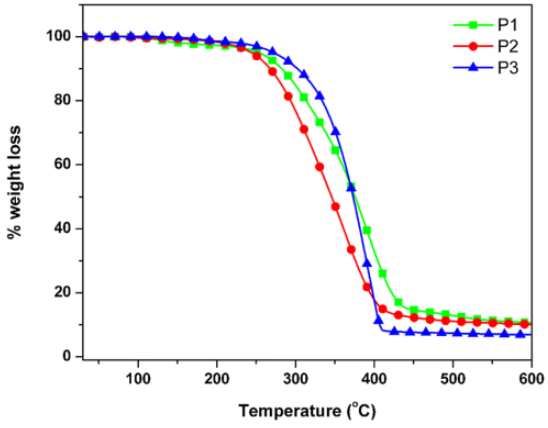

Figure 9. Thermograms of polymers.

Thermal behavior

The onset temperature of polymer degradation exceeded 250°C polymers with a weight loss of 10% between 295°C and 320°C. The polymers exhibited single-step decomposition processes with temperatures between 250°C and 410°C. The temperature of the onset of decomposition for **P3** was higher than that of **P1**, which indicated that the thermal stability of the polymers increases marginally as the alkyl branch increases.

DSC curves exhibited the phase transition of the polymers on heating. Table 3 presents the details of thermal

parameters, and Figure 9 shows the thermograms. A thermal transition in relation to the glass transition temperature (T_g) was observed above 100°C. The synthesized polymers showed T_g between 125°C and 138°C. Normally, the T_g of PFs tends to be around 50°C.[60] The significantly high T_g may be due to the introduction of anthracene in the polymer chain, which contributed to the formation of a bridged 3D network that improved the chain's stiffness. The addition of alkyl DPA into the polymer thus provides higher T_g and thermal stability, which is ideal for it to be used for display purposes as an active layer.

Thus, the addition of alkyl-substituted DPA in the polymer chain together with aniline containing fluorene forms a 3D cross-linked structure resulting in good thermal stability. This prevents deformation and aggregation in the polymer layer from occurring due to heat generated during device operation.

X-Ray diffraction

X-Ray diffraction study is performed to study the crystalline nature of the polymers. As crystallinity defines the degree of long-range order in a material and strongly affects its important properties. T_g of the polymers, which is an important factor for light-emitting polymers, is also dependent on the crystallinity. The crystallite size was determined for all polymers using the Debye–Scherrer equation and was obtained within 0.297–2.89 Å, as given in Table S1. The polymers were partially crystalline, which can be seen from their diffractograms, as shown in Figure S2. All polymers showed small, well-resolved peaks of different intensities in their diffractograms. Peaks in the diffractogram of **P1** were more intense, suggesting more crystalline nature. The small broadening of the area below the peaks was also noticeable in diffractograms of polymers, which could be due to the partially crystalline nature of the polymers, but the broadening area observed for **P2** and **P3** was more than **P1**, indicating the presence of slight amorphous content in their structure, which was also evident from their polymer crystallite sizes.

Conclusion

Overall a low-cost copper-catalyzed Ullmann coupling, which is more economical for mass production, PFs containing anthracene were synthesized in good yields. The polymers obtained were high in molecular weight. So, catalytic polymerization could be achieved using cheap copper as an alternative. The anthracene alkyl groups have very little effect on the polymer absorption, emission, and electrochemical properties. Because of rigid structure and steric hindrance, aggregation was greatly reduced with the addition of phenylamine groups on fluorene. The electrochemical study showed that the values of HOMO and LUMO were similar to those of the commonly used hole-transporting materials. Thermal studies showed decomposition at high temperatures and the polymers exhibited significant thermal stability. All the data collected for PFs indicated that these copolymers could be useful for use in organic electronics as hole-transporting materials, thereby confirming that copper can be effectively used as a catalyst for producing high-performance polymers for organic electronics.

Declaration of conflicting interests

The author(s) declared no potential conflicts of interest with respect to the research, authorship, and/or publication of this article.

Funding

The author(s) received no financial support for the research, authorship, and/or publication of this article.

ORCID iD

Vishwanath R Patil https://orcid.org/0000-0002-3606-9670

Supplemental material

Supplemental material for this article is available online.

References

1. Burroughes JH, Bradley DDC, Brown AR, et al. Light-emitting diodes based on conjugated polymers. *Nature* 1990; **347**: 539–541.
2. AlSalhi MS, Alam J, Dass LA, et al. Recent advances in conjugated polymers for light emitting devices. *Int J Mol Sci* 2011; **12**: 2036.
3. Vacareanu L, Ivan T and Grigoras M. New symmetrical conjugated thiophene-azomethines containing triphenylamine or carbazole units: synthesis, thermal and optoelectrochemical properties. *High Perform Polym* 2012; **24**: 717–729.
4. Facchetti A. π-Conjugated polymers for organic electronics and photovoltaic cell applications. *Chem Mater* 2010; **23**: 733–758.
5. Moliton A and Hiorns RC. Review of electronic and optical properties of semiconducting π-conjugated polymers: application in optoelectronics. *Polym Int* 2004; **53**: 1397.
6. Virgili T, Lidzey DG and Bradley DDC. Efficient energy transfer from blue to red in tetraphenylporphyrin-doped poly(9,9-dioctylfluorene) light-emitting diodes. *Adv Mater* 2000; **12**: 58.
7. Lane PA, Palilis LC, O'Brien DF, et al. Origin of electrophosphorescence from a doped polymer light emitting diode. *Phys Rev B* 2001; **63**: 206–235.
8. Donat-Bouillud A, Levesque I, Tao Y, et al. Organic tunable electroluminescent diodes from polyfluorene derivatives. *Chem Mater* 2000; **12**: 1931–1936.
9. Zhou S, Jia D and Liu J. Synthesis and characterization of novel cross-linking light-emitting polyfluorene derivatives. *High Perform Polym* 2015; **27**: 226–232.

10. Wang S, Oldham WJ, Hudack RA, et al. Synthesis, morphology, and optical properties of tetrahedral oligo(phenylenevinylene) materials. *Am Chem Soc* 2000; **122**: 5695–5709.
11. Zotti G, Schiavon G, Zecchin S, et al. Influence of residual catalyst on the properties of conjugated polyphenylenevinylene materials: palladium nanoparticles and poor electrical performance. *Macromolecules* 2002; **35**: 2122–2135.
12. Ofer D, Swager TM and Wrighton MS. Solid-state ordering and potential dependence of conductivity in poly (2,5-dialkoxy-p-phenyleneethynylene). *Chem Mater* 1995; **7**: 8–425.
13. Zhou Q and Swager TM. Fluorescent chemosensors based on energy migration in conjugated polymers: the molecular wire approach to increased sensitivity. *J Am Chem Soc* 1995; **117**: 12593–12602.
14. Ramos AM, Rispens MT, Van Duren JKJ, et al. Photoinduced electron transfer and photovoltaic devices of a conjugated polymer with pendant fullerenes. *J Am Chem Soc* 2001; **123**: 6714–6715.
15. Lère-Porte JP, Moreau JJE and Torreilles C. Highly conjugated poly (thiophene)s-synthesis of regioregular 3-alkylthiophene polymers and 3-alkylthiophene/thiophene copolymers. *Eur J Org Chem* 2001; **2001**: 1249–1258.
16. Dhanabalan A, Van Dongen JLJ, Van Duren JKJ, et al. Synthesis, characterization, and electrooptical properties of a new alternating. *N*-dodecylpyrrole–benzothiadiazole copolymer. *Macromolecules* 2001; **34**: 2495–2501.
17. Wang F, Wilson MS, Rauh RD, et al. Electroactive and conducting star-branched poly(3-hexylthiophene)s with a conjugated core. *Macromolecules* 1999; **32**: 4272–4278.
18. Yamamoto T, Hayashi Y and Yamamoto A. A novel type of polycondensation utilizing transition metal catalysed C-C coupling. *Bull Chem Soc Jpn* 1978; **51**: 2091–2097.
19. Nurulla I, Morikita H, Fukumoto H, et al. Preparation and properties of poly[(2- alkylbenzimidazole)-alt-thiophene]s with long alkyl side chains. *Macromol Chem Phys* 2001; **202**: 2335–2340.
20. Misumi Y and Masuda T. Living polymerization of phenylacetylene by novel rhodium catalysts. quantitative initiation and introduction of functional groups at the initiating chain end. *Macromolecules* 1998; **31**: 7572–7573.
21. Misumi Y, Kanki K, Miyake M, et al. Living polymerization of phenylacetylene by isolated rhodium. *Macromol Chem Phys* 2000; **201**: 2239–2244.
22. Kishimoto Y, Eckerle P, Miyatake T, et al. Well-controlled polymerization of phenylacetylenes with organorhodium(I) complexes: mechanism and structure of the polyenes. *Am Chem Soc* 1999; **121**: 12035–12044.
23. Osedach TP, Andrew TL and Bulovic V. Effect of synthetic accessibility on the commercial viability of organic photovoltaics. *Energy Environ Sci* 2013; **6**: 711–718.
24. Burke DJ and Lipomi DJ. Green chemistry for organic solar cells. *Energy Environ Sci* 2013; **6**: 2053–2066.
25. Neher D. Polyfluorene homopolymers: conjugated liquid crystalline polymers for bright blue emission and polarized electroluminescence. *Macromol Rapid Commun* 2001; **22**: 1365–1385.
26. Tsami A, Yang XH, Galbrecht F, et al. Enhancing the device performance of a blue light-emitting copolymer using CdSe/ZnS quantum dots. *J Polym Sci A Polym Chem* 2007; **45**: 4773–4785.
27. Tsami A, Yang XH, Farrell T, et al. Alternating fluorene-di(thiophene)quinoxaline copolymers via microwave-supported Suzuki cross-coupling reactions. *J Polym Sci A Polym Chem* 2008; **46**: 7794–7808.
28. List EJW, Guentner R, Freitas PS, et al. The effect of Keto defect sites on the emission properties of polyfluorene-type materials. *Adv Mater* 2002; **14**: 374–378.
29. Sims M, Bradley DC, Ariu M, et al. Understanding the origin of the 535 nm emission band in oxidized poly(9,9-dioctylfluorene): the essential role of inter-chain/intersegment interaction. *Adv Funct Mater* 2004; **14**: 765–781.
30. An BK, Kim YH, Shin DC, et al. Efficient and bright blue electroluminescence of poly[4,4′-biphenylene-α-(9″,9″-dihexyl-3-fluorenyl)vinylene]. *Macromolecules* 2001; **34**: 3993–3997.
31. Casalbore-Miceli G, Esposti AD, Fattori V, et al. A correlation between electrochemical properties and geometrical structure of some triarylamines used as hole transporting materials in organic electroluminescent devices. *Phys Chem Chem Phys* 2004; **6**: 3092–3096.
32. Huang Q, Li J, Evmenenko GA, et al. Systematic investigation of nanoscale adsorbate effects at organic light-emitting diode interfaces. Interfacial structure-charge injection-luminance relationships. *Chem Mater* 2006; **18**: 2431–2442.
33. Huang Q, Cui J, Veinot GC, et al. Realization of high-efficiency/high-luminance small-molecule organic light-emitting diodes: synergistic effects of siloxane anode functionalization/hole-injection layers, and hole/exciton-blocking/electron-transport layers. *Appl Phys Lett* 2003; **82**: 331–333.
34. Jou JH, Sun MC, Chou HH, et al. Efficient pure-white organic light-emitting diodes with a solution-processed, binary-host employing single emission layer. *Appl Phys Lett* 2006; **88**: 141101–141103.
35. Thomas KRJ, Velusamy M, Lin JT, et al. Hexaphenylphenylene dendronised pyrenylamines for efficient organic light-emitting diodes. *J Mater Chem* 2005; **15**: 4453–4459.
36. Yi H, Iraqi A, Stevenson M, et al. A new class of blue-emitting materials for LED applications: triarylamine N-functionalised 2,7-linked carbazole polymers. *Macromol Rapid Commun* 2007; **28**: 1155–1160.
37. Kobayashi N, Koguchi R and Kijima M. Novel blue light emitting poly(N-arylcarbazol-2,7-ylene) homopolymers: syntheses and properties. *Macromolecules* 2006; **39**: 9102–9111.
38. Becker HD. Unimolecular photochemistry of anthracenes. *Chem Rev* 1993; **93**: 145–172.
39. Agbandje M, Jenkins TC, McKenna R, et al. Anthracene-9, 10-diones as potential anticancer agents. Synthesis, DNA-

binding, and biological studies on a series of 2, 6-disubstituted derivatives. *J Med Chem* 1992; **35**: 1418–1429.
40. Inoue Y, Tokito S, Ito K, et al. Perfluoropentacene: high-performance p-n junctions and complementary circuits with pentacene. *J Appl Phys* 2004; **95**: 5795–5799.
41. Chung DS, Park JW, Park JH, et al. High mobility organic single crystal transistors based on soluble triisopropylsilylethynyl anthracene derivatives. *J Mater Chem* 2010; **20**: 524–530.
42. Kim SH, Kim JH, Park S, et al. Highly efficient and stable deep-blue emitting anthracene-derived molecular glass for versatile types of non-doped OLED applications. *J Mater Chem* 2012; **22**: 123–129.
43. Kondakov DY. Role of chemical reactions of arylamine hole transport materials in operational degradation of organic light-emitting diodes. *J Appl Phys* 2007; 102: **114504**.
44. Chiang CJ, Kimyonok A, Etherington MK, et al. Ultrahigh efficiency fluorescent single and bi-layer organic light emitting diodes: the key role of triplet fusion. *Adv Funct Mater* 2013; **23**: 739–746.
45. Nasu K, Nakagawa T, Nomura H, et al. A highly luminescent spiro-anthracenone-based organic light-emitting diode exhibiting thermally activated delayed fluorescence. *Chem Commun* 2013; **49**: 10385–10387.
46. Hasija DC, Gopalakrishnan J, Mishra AV, et al. Exploring copper as a catalyst for cost effective synthesis of polyfluorenes: an alternative to platinum and palladium. *SN Appl Sci* 2020; **2**: 569.
47. Mishra AV, Hasija DC and Patil VR. Novel blue-emitter-containing *o*-terphenyl-substituted fluorene and diphenylanthracene units. *ChemistrySelect* 2018; **3**: 13665–13669.
48. Gopalakrishnan J, Hasija DC and Patil VR. Synthesis, photophysical studies of blue-light-emitting alternating polymers from substituted 9-sila fluorenes and substituted *p*-phenylacene. *ChemistrySelect* 2020; **5**: 2577–2580.
49. Ding JQ, Lu JH, Cheng YX, et al. Manipulating charges and excitons within a single-host system to accomplish efficiency/CRI/color-stability trade-off for high-performance OWLEDs. *Adv Funct Mater* 2008; **18**: 2754–2762.
50. Yang J, Cheng H and Frost RL. Synthesis and characterisation of cobalt hydroxy carbonate $CO_2CO_3(OH)_2$ nanomaterials. *Spectrochim Acta A* 2011; **78**: 420–428.
51. Barve KA, Raut SS, Mishra AV, et al. Synthesis and studies of blue light emitting polymers containing triphenylamine-substituted fluorene and diphenylanthracene moiety. *J Appl Polym Sci* 2011; **122**: 3483–3492.
52. Chalke RM and Patil VR. New approaches towards the synthesis and characterization of alkoxy substituted spirobifluorenes and spirosilabifluorenes for organic optoelectronics. *J Macromol Sci A* 2017; **54**: 556–564.
53. Chalke RM and Patil VR. Novel methoxy spirobifluorene and alkyl substituted diphenylacene based organic blue light emitting polymers for application in organic electronics. *Polymer* 2017; **123**: 355–365.
54. Hwang DH, Park MJ, Lee JH, et al. Synthesis and light-emitting properties of polyfluorene copolymers containing a hydrazone derivative as a comonomer. *Synthetic Metals* 2004; **146**: 145–150.
55. Chou CH, Hsu SL, Dinakaran K, et al. Synthesis and characterization of luminescent polyfluorenes incorporating side-chain-tethered polyhedral oligomeric silsesquioxane units. *Macromolecules* 2005; **38**: 745–751.
56. Maiti D and Buchwald LS. Cu-catalyzed arylation of phenols: synthesis of sterically hindered and heteroaryl diaryl ethers. *J Org Chem* 2010; **75**: 1791–1794.
57. Klarner G, Davey MH, Chen MD, et al. Colorfast blue-light-emitting random copolymers derived from Di-*n*-hexylfluorene and anthracene. *Adv Mater* 1998; **10**: 993.
58. Tokito S, Weinfurtner K, Fujikawa H, et al. Acene containing polyfluorenes for red, green and blue emission in organic light-emitting diodes. *Org Light Emit Mater Dev IV* 2001; **4105**: 69–74.
59. Agarwal N. The synthesis and characterization of photonic materials composed of substituted fluorene donors and a porphyrin acceptor. *Dyes Pigm* 2009; **83**: 328–333.
60. Ding JF, Day M, Robertson G, et al. Electrochemical and fluorescent properties of alternating copolymers of 9,9-dioctylfluorene and oxadiazole as blue electroluminescent and electron transport materials. *J Macromol* 2002; **35**: 3474.